



Quark-diquark models and baryonic fluctuations in QCD *

E. Megías^{a,1}, E. Ruiz Arriola^a, L. L. Salcedo^a^a*Departamento de Física Atómica, Molecular y Nuclear and Instituto Carlos I de Física Teórica y Computacional, Universidad de Granada, Avenida de Fuente Nueva s/n, 18071 Granada, Spain*

Abstract

We study the baryonic fluctuations of electric charge, baryon number and strangeness, by considering a realization of the Hadron Resonance Gas model in the light flavor sector of QCD. We elaborate on the idea that the susceptibilities can be saturated with excited baryonic states with a quark-diquark structure with a linearly confining interaction identical up to a constant to the quark-antiquark potential, $V'_{qD}(r) = V'_{q\bar{q}}(r)$. We obtain an overall good agreement with the spectrum obtained with other quark models and with lattice data for the fluctuations.

Keywords: finite temperature QCD, fluctuations, quark models, missing states, Polyakov loop

1. Introduction

In recent years, the thermodynamic approach to strong interactions pioneered by Hagedorn [1, 2] where the vacuum is represented by a non-interacting Hadron Resonance Gas (HRG), has been used intensively to study the thermodynamics of the confined phase of Quantum Chromodynamics (QCD). One of the greatest achievements of this approach has been the recent study of the trace anomaly, $(\epsilon - 3P)/T^4$ with ϵ energy density and P the pressure. It was computed directly in lattice QCD by several collaborations [3, 4] and within the HRG approach by using the most recent compilation of the hadronic states by the Particle Data Group (PDG) [5], leading to an excellent agreement for temperatures below $T \sim 170$ MeV (see e.g. Ref. [6] and references therein). Thus, this approach has emerged as a practical and viable path to establish completeness of hadronic states in the hadronic phase [7–9].

There are a number of quark models that try to compute the hadron spectrum, one of the most fruitful being

the Relativized Quark Model (RQM) for mesons [10] and baryons [11]. This model shows that there are *further states* in the spectrum above some scale as compared to the PDG, that may be confirmed in the future as hadrons, although they could also be exotic, glueballs or hybrid states. On the other hand, the suspicion that the baryonic spectrum can be understood in terms of quark-diquark degrees of freedom [12] has motivated the use of diquark models. Lattice QCD has also provided insights, as some evidence on diquarks correlations in the nucleon [13] and the dominance of the scalar diquark channel [14] have been reported. Previous studies have traditionally focused on the *individual* one-to-one mapping of resonance states [15]. In contrast, the thermodynamic approach allows to perform a more global analysis of the spectrum, so that possible fine and hyperfine interaction terms are not relevant.

Apart from the equation of state, there are also other thermal observables, like the fluctuations of conserved charges [16], that can be used to study the QCD spectrum by distinguishing between different flavor sectors. In the present work, we profit from the new perspective provided by lattice QCD based on the separation of quantum numbers, and try to answer the question whether or not quark-diquark states saturate the baryonic susceptibilities below the deconfinement crossover.

*Talk given at 22th International Conference in Quantum Chromodynamics (QCD 19), 2 - 5 July 2019, Montpellier - FR

Email addresses: emegias@ugr.es (E. Megías), earriola@ugr.es (E. Ruiz Arriola), salcedo@ugr.es (L. L. Salcedo)

¹Speaker, Corresponding author.

2. QCD spectrum and thermodynamics

The cumulative number of states is very useful for the characterization of the QCD spectrum. It is defined as the number of bound states below some mass M , i.e.

$$N(M) = \sum_i g_i \Theta(M - M_i), \quad (1)$$

where M_i is the mass of the i th hadron, g_i is the degeneracy, and $\Theta(x)$ is the step function. So far, the states listed in the PDG echo the standard quark model classification for mesons $[q\bar{q}]$ and baryons $[qqq]$. Then, it would be pertinent to consider also the spectrum of the RQM for hadrons, as it corresponds *by construction* to a solution of the quantum mechanical problem for both $q\bar{q}$ -mesons and qqq -baryons. For color-singlet states, the n -parton Hamiltonian takes the form

$$H_n = \sum_{i=1}^n \sqrt{p_i^2 + m^2} + \sum_{i<j}^n v_{ij}(r_{ij}), \quad (2)$$

where the two-body interactions take the form $v_{q\bar{q}}(r) = -4\alpha_S/(3r) + \sigma r = (N_c - 1)v_{qq}(r)$. This Hamiltonian for $n = 2(3)$ describes the underlying dynamics of mesons(baryons). A semiclassical expansion of the cumulative number of states [17] can be used to study the high mass spectrum for systems where interactions are dominated by linearly rising potentials with a string tension σ , in the range $M \gg \sqrt{\sigma}$. At leading order in the expansion, the cumulative number takes the form

$$N_n(M) \sim g_n \int \prod_{i=1}^n \frac{d^3 x_i d^3 p_i}{(2\pi)^3} \delta\left(\sum_{i=1}^n \mathbf{x}_i\right) \delta\left(\sum_{i=1}^n \mathbf{p}_i\right) \times \theta(M - H_n(p, x)) \sim \left(\frac{M^2}{\sigma}\right)^{3n-3}, \quad (3)$$

where in the last equality we have neglected the Coulomb term of the potential. Then, one can predict that the large mass expansion of these contributions is

$$N_{[q\bar{q}]} \sim M^6, \quad N_{[qqq]} \sim M^{12}, \quad N_{[q\bar{q}q\bar{q}]} \sim M^{18}, \dots \quad (4)$$

We display in Fig. 1 the separate contributions of meson and baryon spectra for the PDG and RQM. Note that while in the meson case the $N_{[q\bar{q}]} \sim M^6$ behavior seems to conform with the asymptotic estimate, in the baryon case much lower powers, $M^6 - M^8$, than the expected one are identified. We note that M^6 suggests a two-body dynamics, and we take this feature as a hint that the qqq excited spectrum effectively conforms to a two body system of particles interacting with a linearly growing potential. The consequences of this picture will be analyzed in Sec. 4.

3. Fluctuations of conserved charges in a thermal medium

Conserved charges $[Q_a, H] = 0$ play a fundamental role in the thermodynamics of QCD. In the (uds) flavor sector, the conserved charges are the electric charge Q , the baryon number B , and the strangeness S . Their thermal expectation values in the hot vacuum are vanishing, but they present statistical fluctuations that can be computed from the grand-canonical partition function [18]

$$Z_{\text{QCD}} = \text{Tr} \exp \left[- \left(H_{\text{QCD}} - \sum_a \mu_a Q_a \right) / T \right]. \quad (5)$$

By differentiation with respect to the chemical potentials, one finds the susceptibilities

$$\chi_{ab}(T) \equiv \frac{1}{VT^3} \langle \Delta Q_a \Delta Q_b \rangle_T, \quad \Delta Q_a = Q_a - \langle Q_a \rangle_T, \quad (6)$$

where $Q_a \in \{Q, B, S\}$. QCD at high temperature behaves as an ideal gas of quarks and gluons, and in this limit the susceptibilities approach

$$\chi_{ab}(T) \xrightarrow{T \rightarrow \infty} \frac{N_c}{3} \sum_{i=1}^{N_f} q_i^a q_i^b, \quad (7)$$

where $q_i^a \in \{Q_i, B_i, S_i\}$. Within the HRG approach, the charges are carried by various species of hadrons, so that $Q_a = \sum_i q_i^a N_i$, where N_i is the number of hadrons of type i . This approach, valid at low enough temperatures, leads to the result [19]

$$\chi_{ab}^{\text{HRG}}(T) = \frac{1}{2\pi^2} \sum_{i \in \text{Hadrons}} g_i q_i^a q_i^b \sum_{n=1}^{\infty} \zeta_i^{n+1} \frac{M_i^2}{T^2} K_2 \left(\frac{nM_i}{T} \right), \quad (8)$$

where $\zeta_i = \pm 1$ for bosons and fermions, respectively, and $K_2(x)$ is the Bessel function of the second kind. This equation predicts the asymptotic behavior

$$\chi_{ab}(T) \underset{T \rightarrow 0}{\sim} e^{-M_0/T}, \quad (9)$$

where M_0 is the mass of the lowest-lying state in the spectrum with quantum numbers a and b . This observation makes it appealing to plot the lattice data for the fluctuations in a logarithmic scale. These plots are shown in Fig. 2, and compared with the HRG approach including the RQM spectrum. We also display the result by using the spectrum of the quark-diquark model that is computed in Sec. 4. In the following we will focus on the baryonic susceptibilities, i.e. χ_{BB} , χ_{BQ} and χ_{BS} ; as the quark-diquark picture can only be used to compute the baryon spectrum.

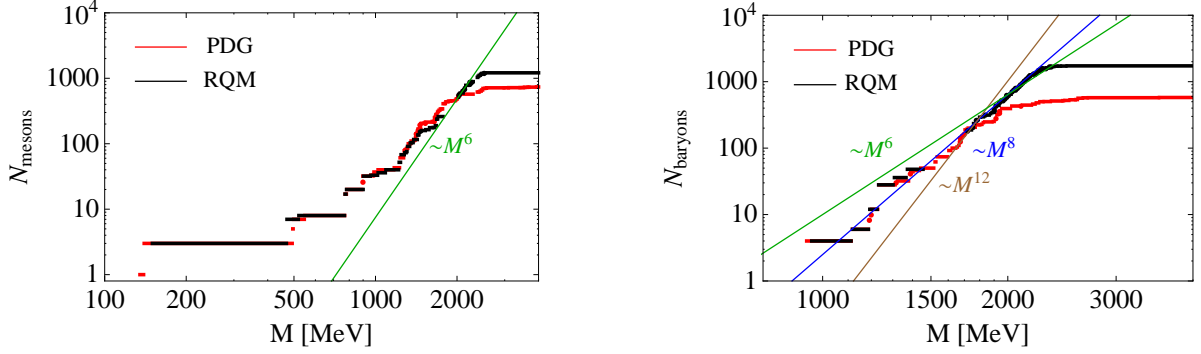


Figure 1: Cumulative numbers for the PDG (red line) and the RQM (black line). We display in log-log scale the mesonic states (left panel), and the baryonic states (right panel).

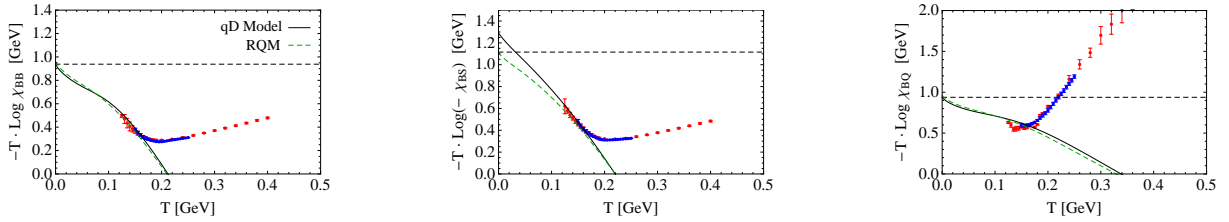


Figure 2: Plot of $-T \log |\chi_{ab}|$ for the baryonic susceptibilities as a function of temperature. We display as dots the lattice data from Refs. [16] (blue) and [20] (red). We also display the HRG approach results including the spectrum of the RQM [11] (dashed green) and the baryon spectrum from the quark-diquark model computed in Sec. 4 (solid black). Horizontal dashed lines represent the values of the lowest-lying states contributing to the fluctuations, cf. Eq. (9).

4. Quark-diquark model for baryons and fluctuations

There is nowadays some discussion about the most probable spatial configuration of quarks inside baryons. An interesting possibility would be that the quarks are distributed according to an isosceles triangle, leading to an easily tractable class of models, the so-called relativistic quark-diquark (qD) models [15, 21, 22]. We will study in this section a simplified version of these models, and use it to compute the baryon spectrum and the baryonic fluctuations.

4.1. The model

In the quark-diquark models, the baryons are assumed to be composed of a constituent quark q , and a constituent diquark $D \equiv (qq)$. In their relativistic version the Hamiltonian writes [15]

$$H_{qD} = \sqrt{\mathbf{p}^2 + m_q^2} + \sqrt{\mathbf{p}^2 + m_D^2} + V_{qD}(r). \quad (10)$$

Using Polyakov loop correlators and Clebsch-Gordan decomposition, we have proven in the static limit that the quark-diquark potential, $V_{qD}(r)$, coincides with the quark-antiquark potential, $V_{q\bar{q}}(r)$, up to an additive constant [19, 23], a feature which is in marked agreement

with recent lattice studies [24]. Hence, we assume

$$V_{qD}(r) = -\frac{\tau}{r} + \sigma r + \mu, \quad (11)$$

with $\tau = \pi/12$ and $\sigma = (0.42 \text{ GeV})^2$. The parameters of the kinetic terms in Eq. (10) are controlled by: i) the constituent quark mass, m_{cons} , and ii) the current quark mass for the strange quark, \hat{m}_s ; in the following way:

$$m_{u,d} = m_{\text{cons}}, \quad m_s = m_{\text{cons}} + \hat{m}_s. \quad (12)$$

In addition, we can distinguish between two kinds of diquarks: scalar D , and axial vector D_{AV} ; and we consider the natural choice

$$m_{D,\text{ns}} = 2m_{\text{cons}}, \quad m_{D_{AV},\text{ns}} = m_{D,\text{ns}} + \Delta m_D, \quad (13)$$

where the subindex ns refers to diquarks with non-strange quarks. Some studies indicate a mass difference between these diquarks of $\Delta m_D \simeq 0.21 \text{ GeV}$ [25], a value that will be adopted in the following. Finally, the breaking of flavor SU(3) for diquarks will be modeled as

$$m_D = m_{D,\text{ns}} + n_s \hat{m}_s, \quad m_{D_{AV}} = m_D + \Delta m_D, \quad (14)$$

where $n_s = 0, 1, 2$, is the number of s quarks in the diquark. With these assumptions, the only free parameters of the model are m_{cons} , \hat{m}_s and μ . We summarize in

Table 1 the degeneracies of the states predicted by the model, by distinguishing between their electric charges. For baryonic states, $B = 1$ and $S = -n_s$.

| Baryon | $Q = -1$ | $Q = 0$ | $Q = 1$ | $Q = 2$ |
|-----------|----------|---------|---------|---------|
| $[nn]n$ | - | 2 | 2 | - |
| $\{nn\}n$ | 6 | 12 | 12 | 6 |
| $[nn]s$ | - | 2 | - | - |
| $\{nn\}s$ | 6 | 6 | 6 | - |
| $[ns]n$ | 2 | 4 | 2 | - |
| $\{ns\}n$ | 6 | 12 | 6 | - |
| $[ns]s$ | 2 | 2 | - | - |
| $\{ns\}s$ | 6 | 6 | - | - |
| $\{ss\}n$ | 6 | 6 | - | - |
| $\{ss\}s$ | 6 | - | - | - |

Table 1: Spin-isospin degeneracies of the baryonic states within the quark-diquark model. n represents the light flavors u, d . We use $\{q_1 q_2\}$ to denote scalar diquarks, and $[q_1 q_2]$ for axial-vector diquarks.

4.2. Baryon spectrum

The spectrum of the quark-diquark model can be obtained by diagonalizing the Hamiltonian of Eq. (10). The problem does not admit an analytic solution, and we will consider a variational procedure in which the model space is truncated. A convenient basis is that of the 3-dimensional isotropic harmonic oscillator (IHO), which is written in terms of the generalized Laguerre polynomials. The matrix elements of the Hamiltonian are then obtained from

$$\langle n\ell | H_{qD} | n'\ell \rangle = \int_0^\infty dr u_{n\ell}^*(r) u_{n'\ell}(r) V_{qD}(r) + \int_0^\infty dp \hat{u}_{n\ell}^*(p) \hat{u}_{n'\ell}(p) \left[\sqrt{p^2 + m_q^2} + \sqrt{p^2 + m_D^2} \right], \quad (15)$$

where $u_{n\ell}(r)$ and $\hat{u}_{n\ell}(p)$ are the reduced wave functions of the IHO in position and momentum space, respectively [19]. A convenient choice of the parameters of the model,

$$\begin{aligned} m_{D,ns} &= 0.6 \text{ GeV}, & m_{u,d} &= 0.3 \text{ GeV}, \\ \hat{m}_s &= 0.10 \text{ GeV}, & \mu &= -0.459 \text{ GeV}, \end{aligned} \quad (16)$$

leads to the spectrum of baryons that is shown in Fig. 3. We find that below $M < 2400$ MeV the quark-diquark spectrum is in remarkable agreement with the RQM spectrum where quark-diquark correlations are not assumed a priori. Let us mention that it is expected that the quark-diquark picture will be reliable only for excited states, so that in the following we will use the empirical value of the mass for the nucleon, $M_n = 938$ MeV, and apply the quark-diquark model only for the other baryons.

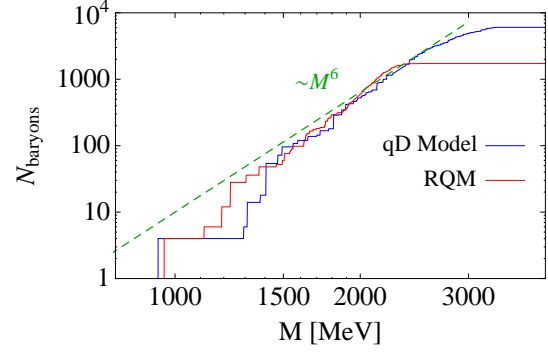


Figure 3: Cumulative number for the spectrum of baryons as a function of the baryon mass. We compare the quark-diquark model of Sec. 4 with parameters in Eq. (16), and the RQM [11].

4.3. Baryonic susceptibilities

From the spectrum of the quark-diquark model, we can obtain the baryonic susceptibilities by using the HRG approach given by Eq. (8). Our goal is to reproduce the lowest temperature values of the lattice results for these quantities. For this purpose we have chosen to minimize the function $\bar{\chi}^2 = \bar{\chi}_{BB}^2 + \bar{\chi}_{BQ}^2 + \bar{\chi}_{BS}^2$, where

$$\bar{\chi}_{ab}^2 = \sum_{j=1}^{j_{\max}} \frac{(\chi_{ab}^{\text{lat}}(T_j) - \chi_{ab}^{\text{HRG}}(T_j))^2}{(\Delta\chi_{ab}^{\text{lat}}(T_j))^2}, \quad (17)$$

and j_{\max} is the number of data points used in the fits. A typical fit of the model prediction with lattice data leads to the values of the parameters presented in Eq. (16), and the corresponding results for the susceptibilities are shown in Fig. 4. In order to perform the best fit to the data, we can study the variation of $\bar{\chi}^2$ in the full parameter space of the model. We show in Fig. 5 a plot of $\bar{\chi}^2/\nu$, where ν is the number of degrees of freedom, in the plane $(\hat{m}_s, m_{\text{cons}})$. One can observe that the current quark mass for the strange quark takes a value compatible with the PDG, i.e., $80 \text{ MeV} \lesssim \hat{m}_s \lesssim 120 \text{ MeV}$. In addition, while the constituent quark mass cannot be determined with precision, we can ensure that it is in the regime $100 \text{ MeV} \lesssim m_{\text{cons}} \lesssim 400 \text{ MeV}$. Typical values of the parameter μ entering in Eq. (11) are in the range $-0.7 \text{ GeV} \lesssim \mu \lesssim 0 \text{ GeV}$.

Some alternative fits have been presented in Ref. [19]. For instance, if the value $\hat{m}_s = 0.10 \text{ GeV}$ is adopted and $m_{D,ns} = 2m_{\text{cons}}$ is not assumed, one finds that the most probable scalar diquark mass is of the order $m_{D,ns} \simeq 0.4 - 0.6 \text{ GeV}$, and the constituent quark mass $m_{\text{cons}} \simeq 0.3 \text{ GeV}$. However, these conclusions depend on the choice of \hat{m}_s , leading to lower values of $m_{D,ns}$ and m_{cons} when \hat{m}_s increases. By using the spectrum of the quark-diquark model, it has been studied in

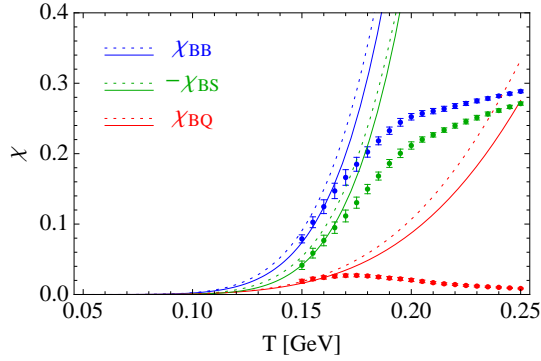


Figure 4: Baryonic susceptibilities from the quark-diquark model (solid) compared to the lattice data of Ref. [16]. We display also as dotted lines the results from the spectrum of the RQM [11]. For the quark-diquark model we have used the parameters in Eq. (16).

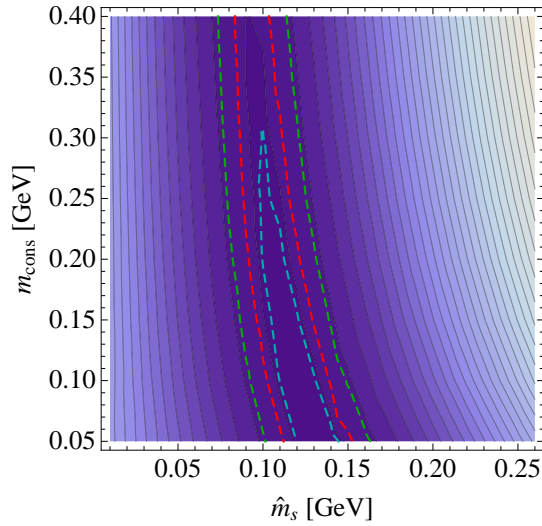


Figure 5: $\bar{\chi}^2/\nu$ in the plane $(\hat{m}_s, m_{\text{cons}})$ from a fit to the lattice data of the baryonic fluctuations from [16] with $T \leq 165$ MeV. The dashed lines correspond to $\bar{\chi}^2/\nu = 0.77$ (blue), $\bar{\chi}^2/\nu = 1$ (red), and $1 + \sqrt{2}/\nu$ (green).

Ref. [19] some of the baryonic fluctuations of fourth order as well. While the agreement with lattice data is reasonable, these data are typically affected by larger error bars than those of the second-order fluctuations; hence, no firm conclusions can be extracted from a fit to these quantities.

5. Conclusions

In the present work we have studied the baryonic susceptibilities in a thermal medium in the (uds) flavor sector of QCD by using the HRG approach. Being the predictions of this model sensitive to the spectrum of QCD, this study is also relevant for the characterization of the spectrum and its completeness. In particular, we

have argued that the asymptotic three-body phase space for confined qqq systems $\sim M^{12}$ is much larger than the one actually determined in the RQM, $\sim M^6$, which resembles instead a two body systems. This strongly suggests a dominance of quark-diquark dynamics for excited baryons, motivating the use of a quark-diquark model to compute the baryon spectrum. The free model parameters: constituent quark mass, current quark mass for the strange quark, and an additive constant entering in the quark-diquark potential; have been determined from a fit of the baryonic susceptibilities with lattice data. The results are reasonable and fall in the bulk of previous intensive studies where a detailed description of the spectrum was pursued. The extension of this study to nonbaryonic susceptibilities would require a specific model for mesons which would not be related to the quark-diquark dynamics. These and other issues will be addressed in a forthcoming publication [26].

Acknowledgements

This work is supported by the Spanish MINECO and European FEDER funds (Grants No. FIS2014-59386-P and FIS2017-85053-C2-1-P), Junta de Andalucía (Grant No. FQM-225), and by the Consejería de Conocimiento, Investigación y Universidad of the Junta de Andalucía and European Regional Development Fund (ERDF) (Grant No. SOMM17/6105/UGR). The research of E.M. is also supported by the Ramón y Cajal Program of the Spanish MINECO (Grant No. RYC-2016-20678).

References

- [1] R. Hagedorn, Nuovo Cim. Suppl. **3** (1965) 147–186.
- [2] R. Hagedorn, Lect. Notes Phys. **221** (1985) 53–76.
- [3] S. Borsanyi, Z. Fodor, C. Hoelbling, S. D. Katz, S. Krieg, K. K. Szabo, Phys. Lett. **B730** (2014) 99–104.
- [4] A. Bazavov, et al., Phys. Rev. **D90** (2014) 094503.
- [5] M. Tanabashi, et al., Phys. Rev. **D98** (3) (2018) 030001.
- [6] E. Ruiz Arriola, L. L. Salcedo, E. Megias, Acta Phys. Polon. **B45** (12) (2014) 2407–2454.
- [7] E. Megias, E. Ruiz Arriola and L. L. Salcedo, Phys. Rev. **D94** (9) (2016) 096010.
- [8] E. Ruiz Arriola, W. Broniowski, E. Megias, L. L. Salcedo, YSTAR2016 Mini-Proceedings (2016) 136–147, [arXiv:1612.07091].
- [9] E. Megias, E. Ruiz Arriola, L. L. Salcedo, PoS Hadron2017 (2018) 232.
- [10] S. Godfrey, N. Isgur, Phys. Rev. **D32** (1985) 189–231.
- [11] S. Capstick, N. Isgur, Phys. Rev. **D34** (1986) 2809.
- [12] M. Anselmino, E. Predazzi, S. Ekelin, S. Fredriksson, D. B. Lichtenberg, Rev. Mod. Phys. **65** (1993) 1199–1234.
- [13] C. Alexandrou, P. de Forcrand, B. Lucini, Phys. Rev. Lett. **97** (2006) 222002.

- [14] T. DeGrand, Z. Liu, S. Schaefer, Phys. Rev. **D77** (2008) 034505.
- [15] E. Santopinto, J. Ferretti, Phys. Rev. **C92** (2) (2015) 025202.
- [16] A. Bazavov, et al., Phys. Rev. **D86** (2012) 034509.
- [17] J. Caro, E. Ruiz Arriola, L. Salcedo, J.Phys. **G22** (1996) 981–1011.
- [18] M. Asakawa, M. Kitazawa, Prog. Part. Nucl. Phys. **90** (2016) 299–342.
- [19] E. Megias, E. Ruiz Arriola, L. L. Salcedo, Phys. Rev. **D99** (7) (2019) 074020.
- [20] S. Borsanyi, Z. Fodor, S. D. Katz, S. Krieg, C. Ratti, K. Szabo, JHEP **01** (2012) 138.
- [21] C. Gutierrez, M. De Sanctis, Eur. Phys. J. **A50** (11) (2014) 169.
- [22] P. Masjuan, E. Ruiz Arriola, Phys. Rev. **D96** (5) (2017) 054006.
- [23] E. Megias, E. Ruiz Arriola, L. L. Salcedo, Phys. Rev. **D89** (7) (2014) 076006.
- [24] Y. Koma, M. Koma, Phys. Rev. **D95** (9) (2017) 094513.
- [25] R. L. Jaffe, Phys. Rept. **409** (2005) 1–45.
- [26] E. Megias, E. Ruiz Arriola, L. L. Salcedo, work in progress (2019).